PERGAMON

Journal of Structural Geology 23 (2001) 1933–1952

JOURNAL OF STRUCTURAL GEOLOGY

www.elsevier.com/locate/jstrugeo

Growth and linkage of a segmented normal fault zone; the Late Jurassic Murchison–Statfjord North Fault, northern North Sea

Mike J. Young[a,b,*], Rob L. Gawthorpe[a], Stuart Hardy[a]

[a]*Basin and Stratigraphic Studies Group, Department of Earth Sciences, The University of Manchester, Manchester M13 9PL, UK*
[b]*Present address: Norsk Hydro Produksjon, PO Box 7190, N-5020 Bergen, Norway*

Received 14 August 2000; revised 16 January 2001; accepted 13 February 2001

Abstract

The structure of the 25 km long northeastern portion of the Murchison–Statfjord North Fault Zone and adjacent syn-rift stratigraphy are integrated to reconstruct the temporal and spatial evolution during c. 30.5 myr of Late Jurassic, North Sea rifting. Based on a structural analysis (*D–d* data) alone, approximately 14 precursor fault strands are identified. Incorporation of stratigraphic data shows that only six of these strands were important in controlling stratal architecture and distribution. Three main stages in the evolution of the fault zone are recorded in the syn-rift stratigraphy and are biostratigraphically constrained. These are: (1) following initiation of rifting, six isolated fault strands developed (each <4 km long) and controlled the stratigraphy for c. 13 myr; (2) the isolated strands linked along-strike forming two >9 km long fault segments separated by a 2 km wide relay ramp, that controlled the stratigraphy for at least the following c. 10.5 myr; and (3) the two fault segments hard-linked forming a single, continuous fault trace during the final c. 7 myr of rifting. The results of this study reveal the necessity to adopt an integrated structural and stratigraphic approach when reconstructing the evolution of normal fault zones. The results may also help to further constrain models of fault evolution.

Keywords: Normal faulting; Segmentation; Fault growth and linkage

1. Introduction

In regions of the Earth that have undergone prolonged crustal stretching, extension is usually accommodated on long-lived seismogenic, planar normal faults which bound half-graben sedimentary basins (Jackson et al., 1988). Typically, these fault zones can have lengths in excess of 100 km, but commonly comprise fault traces that are discontinuous along-strike, being composed of individual echelon stepping fault segments that are separated by areas of relatively low displacement (i.e. segment boundaries) or connected by distinct bends in the fault trace. Numerous outcrop and subsurface-based studies have used the structural geometry of the fault trace together with quantitative data sets of fault displacement (*D*) and length (*L*) or distance (*d*), to investigate how fault segments grow and link. In particular, displacement–distance relationships and fault trace geometries have been used to suggest that normal faults develop through the interaction and linkage of individual segments and that evolving faults follow a distinct growth path, as segments progressively link and transfer zones (e.g. relay ramps) break down (Peacock and Sanderson, 1991; Cartwright et al., 1995). Consequently, a number of transient geological structures are believed to characterise specific conceptual stages in the evolution of faults (Table 1).

However, because many studies of normal faults have only used the final disposition of total displacement (e.g. *D–L* characteristics and structural geometry), the temporal growth history cannot be quantified or determined unequivocally. Although there are a number of exceptions (Anders and Schlische, 1994; Schlische, 1995; Gawthorpe et al., 1997; Nicol et al., 1997; Rowan et al., 1998; Contreras et al., 2000; Dawers and Underhill, 2000), the stratigraphy deposited during fault growth has often not been fully utilised, either because it is not present or has not been studied in sufficient detail.

This study integrates structural data from the Murchison–Statfjord North Fault Zone (Fig. 1) with stratigraphic information from the adjacent footwall and hanging wall, to reconstruct the temporal and spatial evolution of this fault zone during c. 30.5 myr of Late Jurassic rifting. This is

* Corresponding author. Tel.: +47-5599-6922; fax: +47-5599-5525.
E-mail address: mike.young@hydro.com (M.J. Young).

0191-8141/01/$ - see front matter
PII: S0191-8141(01)00038-4

Table 1
A summary of geological structures that characterise specific stages in the evolution of normal faults

Fault growth stage		Characteristic structures
1. Isolated fault strands	(i)	Individual fault strands with displacement profiles that decrease from a maximum in the centre to zero at the tips.
	(ii)	Local depocentres in the hanging walls of isolated fault strands are filled by the early syn-rift sequences that have a limit areal extent and are thickest towards the centre of the isolated fault strands.
	(iii)	Fault strands and associated hanging wall depocentres are separated by relative highs; regions that experience displacement deficit rather than displacement transfer. These highs are onlapped by the early syn-rift sequences.
2. Soft-linkage	(i)	Formation of 'ductile structures' such as relay ramps, which transfer displacement between echelon stepping, soft-linked fault strands or segments.
	(ii)	Fault displacement profiles exhibit steep displacement gradients towards transfer zones.
3. 'Break-down' stage	(i)	Strain accumulation in ductile structures reaches critical levels and the structures begin to deform in a brittle manner. Faults begin to cut across relay structures.
4. Hard-linkage	(i)	Transfer faults cut through relay zones linking previously discontinuous fault traces. This results in a single through-going fault that has distinct bends or jogs disrupting the along-strike trend of the fault trace.
	(ii)	The latest syn-rift sequences are thickest towards the centre of hard-linked faults.

achieved through the analysis of a 3-D seismic survey together with well data, providing biostratigraphically defined ages of syn-rift sediments. The structural geometry and displacement–distance (D–d) profile of the fault zone is initially analysed to provide a structural framework and enable general insights to be made into the fault zone evolution. The syn-rift stratigraphy is then examined, especially thickness variations within specific stratal intervals, together with the distribution of seismic stratigraphic units, in order to attempt to reconstruct temporal changes in along-strike displacement, reflecting the segmentation history of the fault zone and the evolving basin topography.

2. Geological setting

The North Sea has experienced two main phases of Mesozoic rifting and associated thermal subsidence, during the Permo-Triassic and the Late Jurassic, separated by a period of thermal doming during the Middle Jurassic (Underhill and Partington, 1993; Underhill, 1998) (Fig. 2). The Late Jurassic phases of rifting resulted in the development of the Viking Graben and East Shetland Basin (Fig. 1), along with the two other arms of the North Sea trilete rift system (Underhill, 1998). This rifting event is believed to overprint and to some extent reactivate earlier

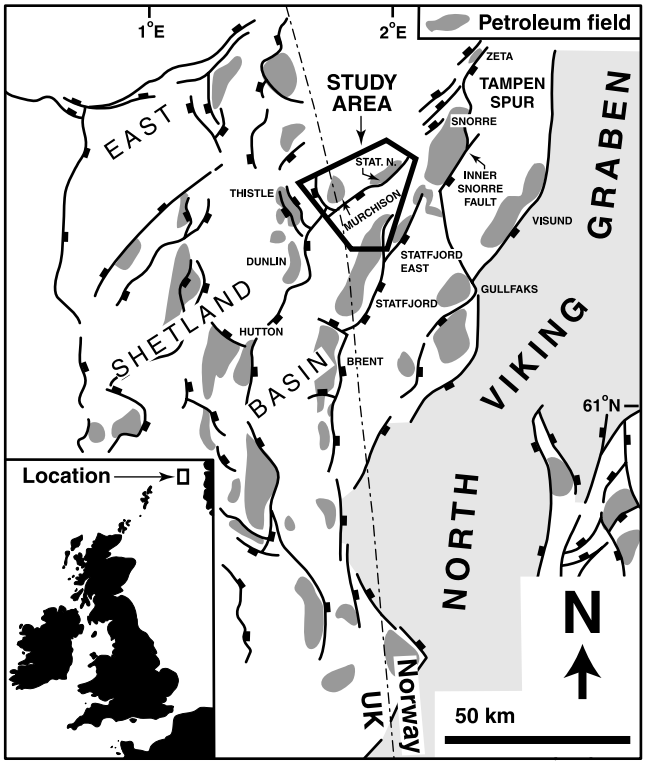

Fig. 1. Location of the study (Murchison-Stratfjord North Fault Zone) in the East Shetland basin, northern North Sea. After Dawers and Underhill (2000).

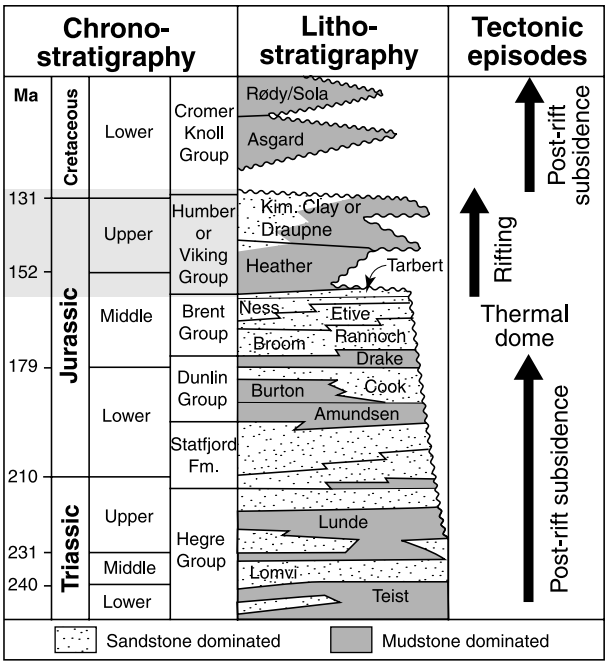

Fig. 2. Stratigraphy and main tectonic events in the Tampen Spur area of the northern North Sea (modified after Dahl and Solli, 1993). Shaded portion of chronostratigraphy is the studied syn-rift interval, which corresponds to the J30–J70 sequences of Rattey and Hayward (1993).

Permo-Triassic rift structures (Færseth, 1996). The Murchison–Statfjord North Fault Zone is situated in the Tampen Spur region of the East Shetland Basin on the western flank of the Viking Graben (Fig. 1). A stretching factor during rifting of approximately 15% (Yielding, 1990; Roberts et al., 1993), associated with a NW–SE to WNW–ESE extension direction, resulted in the formation of major NE–SW-trending predominantly east-dipping normal fault zones (Yielding, 1990).

The onset of extensional activity in the northern North Sea is thought to be marked by the deposition of the Tarbert Formation, the youngest member of the Brent Group (Yielding et al., 1992; Rattey and Hayward, 1993; Ravnås and Bondevik, 1997; Underhill et al., 1997). However, in this region it is the mudstone-dominated Humber Group that represents the majority of the syn-rift stratigraphy, lying above the Brent Group and below the Cretaceous Crommer Knoll Group (Deegan and Scull, 1977). In the Norwegian North Sea, the equivalent of the Humber Group is known as the Viking Group and consists of the Heather Formation and Draupne Formation (equivalent to the Kimmeridge Clay Formation in UK terminology). Both the Heather and Draupne Formations locally contain several internal sandstone units (Fig. 2). In the study area, core data indicate that the syn-rift consists of a mudstone dominated Heather Formation containing turbidite sandstone, overlain by the Draupne Formation consisting of mudstone, turbidite sandstones and shoreface sandstones (Fig. 3). The Late Jurassic sandstones, within the Draupne Formation in the hanging wall of the Murchison–Statfjord North Fault Zone, are known as the Munin Sandstones (Haram et al., 1990; Barnes et al., 1992; Wood and Schwartzbard, 1994).

3. Dataset

The seismic dataset for this study consists of a 3-D survey (named st97m3) around the Murchison and Statfjord North petroleum fields in blocks 33/9, 34/7 (Norwegian sector) and 211/19 (UK sector) of the North Sea (Figs. 1 and 4). The seismic survey covers an area of 25×20 km (i.e. 500 km^2), with line spacing of 12.5 and 18.5 m for in-lines and cross-lines, respectively. The seismic data have a vertical axis in milliseconds (ms) two-way-travel-time (TWT) and have not been depth-converted. Therefore, the results of this study are generally presented with the vertical axis in time. The syn-rift stratigraphy is buried to depth of between 2500 and 3500 ms TWT, and the vertical resolution of the data is estimated to be 10–30 ms TWT (c. 15 to c. 50 m). The wells used in this study to constrain the seismic include six wells (33/9-8, 33/9-14, 33/9-15, 33/9-16, 34/7-20 and 34/7-28) that intersect the syn-rift (Fig. 4a). Seismic horizons were defined at trace positions (i.e. peak, trough, zero-crossing) that tied most closely to formation tops. Results from biostratigraphic and facies studies of the cored intervals of the syn-rift wells (carried out at Saga Petroleum) are incorporated into this study.

Several pre-, syn- and post-rift horizons, constrained by the well data, have been mapped across the study area (Table 2). The horizons were chosen to: (1) allow the geometry and displacement–distance (D–d) characteristics of the fault zone to be established; and (2) determine thickness variations and the internal characteristics of the syn-rift package. The syn-rift package described in this study is defined seismically as that occurring between the top Brent Group and top Draupne Formation (informally known as the 'Base Cretaceous' in the northern North Sea). Seismic reflectors below the top Brent are parallel, whilst reflectors above are non-parallel, define thickness variations and have stratal terminations against the top Brent. The Tarbert Formation is present only in the hanging wall of the Murchison-Stratfjord North Fault Zone, where it is below seismic resolution and generally <15 m thick, as observed within the hanging wall exploration wells. The pre-rift top Statfjord Formation reflector best defines the tectonic structure of the MSNFZ, because it is a high amplitude pre-rift reflector that is free from footwall crest degradation. The top Heather Formation reflector divides the syn-rift into two main seismic units (the Heather and Draupne), whilst predominantly low amplitude seismic reflectors enable the syn-rift to be further subdivided (Table 2). Well data have enabled four seismic surfaces to be dated biostratigraphically. The top Brent Group (top Tarbert in the hanging wall of the MSNFZ) is constrained to be mid-Bathonian, top Heather Formation to be top

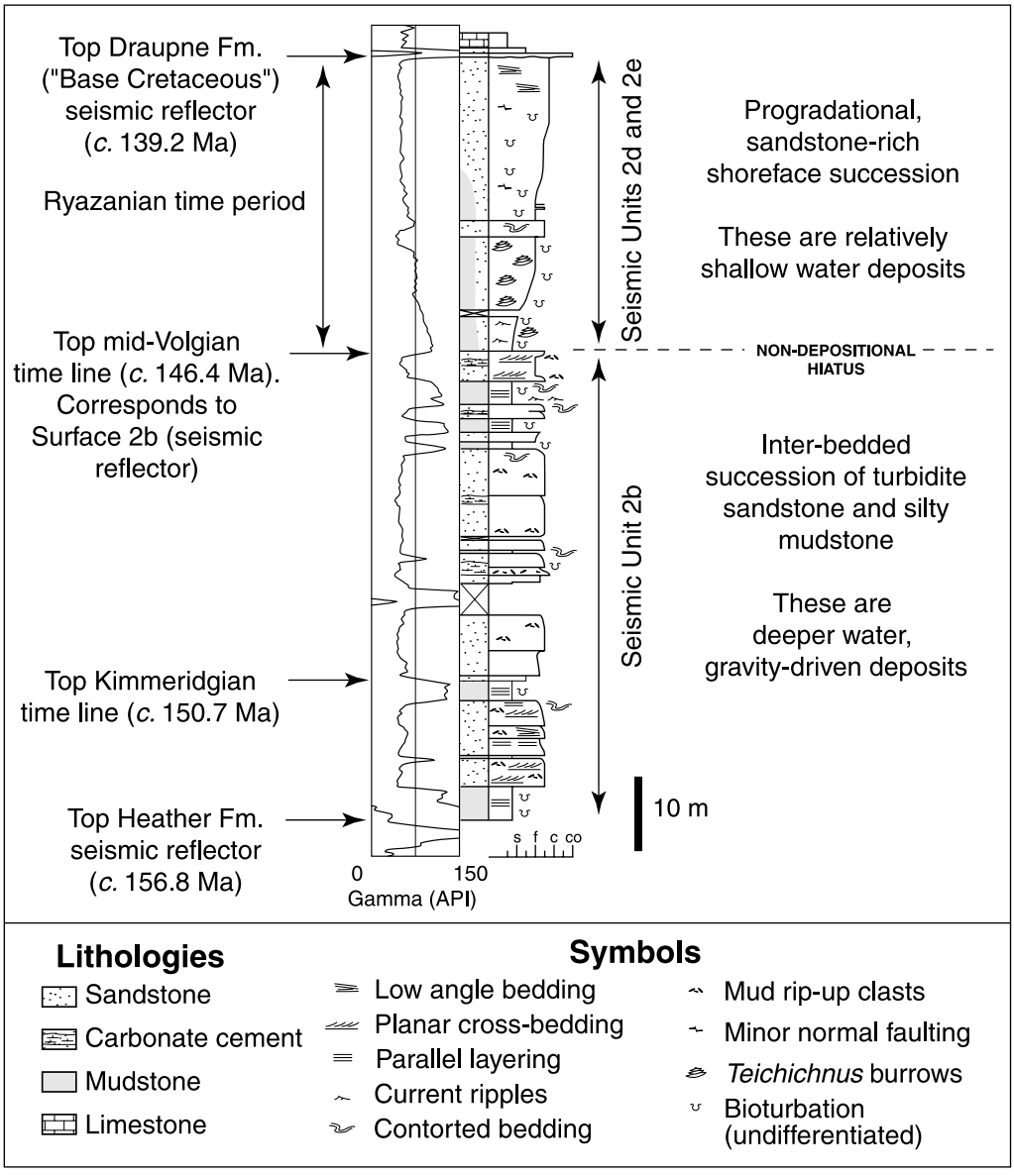

Fig. 3. Log 33/9-15 showing a summary of lithologies, facies, seismic picks and chronostratigraphic markers. Draupne sandstones in the hanging wall of the Murchison-Stratfjord North Fault Zone have previously been termed the Munin Sandstone (Wood and Schwartzbard, 1994). Refer to Fig. 4 for location of the well.

mid-Oxfordian, an intra-Draupne surface (seismic surface 2b; Fig. 5) to be top mid-Volgian, and the top Draupne Formation to be mid/late-Ryazanian.

4. Structure of the Murchison–Statfjord North Fault Zone

4.1. Structural style

The Murchison–Statfjord North Fault Zone (MSNFZ) consists of a NE–SW-trending east-dipping fault with a distinct, 2 km wide jog or bend in the fault trace (Jog Fault) approximately in the middle of the data coverage (Fig. 4). The present day fault trace is continuous for over 40 km (25 km within the study area), from the Dunlin Field in the southwest to the Statfjord North Field, tipping out in the Snorre area to the northeast (Fig. 1). In dip-oriented sections, the Murchison–Statfjord North Fault is planar, with throw varying along-strike between <75 and 450 ms TWT (<c. 120 and c. 710 m). The half-graben, bounded to the northwest by the MSNFZ, pinches out along-strike to the northeast and widens towards the southwest, reaching 9 km in width at the southern end of the data coverage (Fig. 4). In cross-section, the syn-rift, consisting of the Tarbert (although this cannot be proven seismically within the study area), Heather and Draupne Formations, has a broad wedge-shaped geometry showing overall expansion into the fault, and thinning and onlap onto the hanging wall dip-slope towards the southeast (Fig. 5a and b).

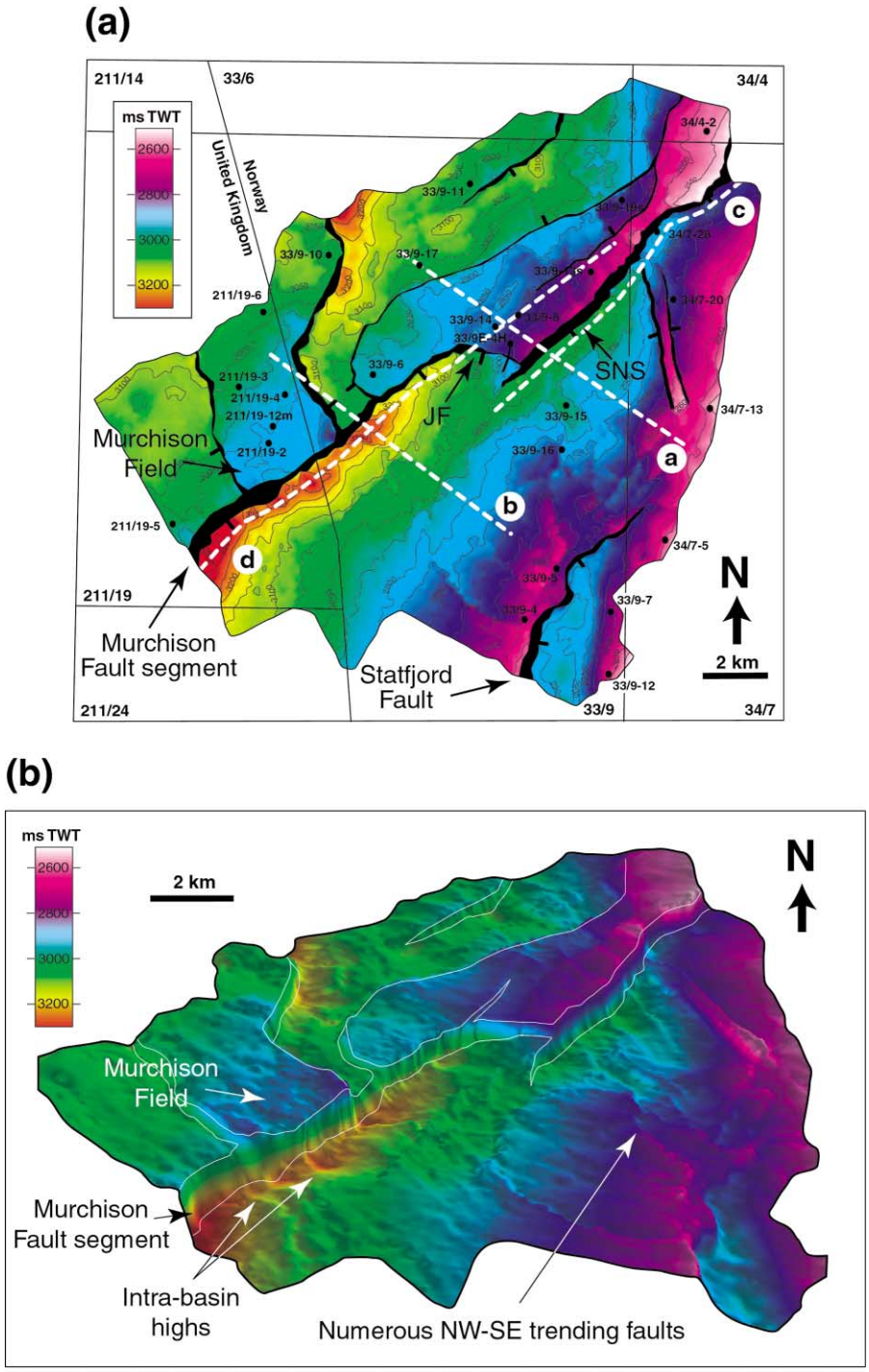

Fig. 4. The structure of the study area at top Statfjord level, in milliseconds two-way-travel time. (a) Plan view map, where ticks indicate down-throw on faults, and a–d refer to the location of seismic lines shown in Fig. 5. (b) 3-D view towards the north, where the main faults are outlined in white (hanging wall and footwall cut-offs of the top Statfjord Formation).

However, in the immediate hanging wall of the fault zone, strata commonly dip to the southeast, into the hanging wall, with the thickest strata occurring in asymmetric synclinal troughs that parallel the strike of the fault zone, and whose fold axes are located up to 1 km basinward (i.e. southeast) of the hanging wall cut-off (Fig. 5a and b). These hanging wall synclines are discontinuous along their lengths, being disrupted by intra-basin highs (Fig. 4). These intra-basin highs can be seen on a strike-parallel seismic traverse within the immediate hanging wall to the MSNFZ as a series of broad folds (affecting the parallel pre-rift strata), with a wavelength up to 5 km and an amplitude up to 150 ms TWT (c. 240 m) (Fig. 5d).

In addition to the major NE–SW-trending MSNFZ, there

Table 2
A summary of the characteristics of the main seismic reflectors used as the basis for this study

Horizon	Amplitude	Continuity	Comments
Top Draupne or top syn-rift ('Base Cretaceous')	Very high	Excellent	Marks the boundary between the high velocity marls/limestones of the Mime Fm. and the relatively low velocity Draupne Fm.
Intra-Draupne Fm. (syn-rift)	Low to moderate	Good to poor	Velocity changes from shale to sandstone or minor velocity changes between shales.
Top Heather Fm. (syn-rift)	Moderate to high	Good	Marks the boundary between low velocity Draupne shales and higher velocity Heather shales.
Intra-Heather Fm. (syn-rift)	Low to moderate	Moderate to poor	Minor velocity changes between shales.
Top Brent Gp. (base syn-rift)	Moderate to high	Good	Marks the boundary between Heather shale and the underlying Tarbert Fm., resulting in a slight increase in acoustic impedance.
Top Statfjord Fm. (pre-rift)	Generally high	Good	Marks the boundary between the high velocity calcareous beds of the Amundsen Fm. and the sandstone beds of the Statfjord Fm.

are a series of NW–SE-trending faults within the study area that generally have a maximum displacement <50 ms TWT (<c. 75 m) and length <6 km (Fig. 4). In the hanging wall of the MSNFZ, there are several minor faults that splay off the fault plane and extend <2 km into the hanging wall before they tip out (Fig. 4). There are also a series of faults that fan from the footwall of the Statfjord Fault and tip out towards the MSNFZ (Fig. 4).

The footwall structure of the MSNFZ is generally simple, consisting of planar (without any clear folds), parallel pre-rift (Triassic to Middle Jurassic) strata that dip towards the northwest and abut against the fault plane or are locally eroded (Fig. 5a). In the footwall (and hanging wall) to the Jog Fault the pre-rift strata dip towards the southwest (Figs. 4 and 5d). Erosion of the footwall crest is common along the length of the fault zone, largely affecting the Brent Group, and typically eroding <500 m back from the projected position of the footwall crest. The erosion commonly produces a scoop-shaped cut in the top of the fault plane, which is onlapped predominantly by the syn-rift strata (e.g. Fig. 5a and b). This is comparable to the process of fault scarp degradation seen along the crest of numerous footwalls in the northern North Sea, such as Ninian (Underhill et al., 1997) and Brent (McLeod and Underhill, 1999). There are a number of NW–SE-trending faults in the footwall with maximum displacements <175 ms TWT (<c. 280 m) and lengths >6 km, which terminate against the MSNFZ and do not cross into the hanging wall (Fig. 4). It is difficult to date the movement on these footwall faults as there is rarely significant syn-rift present. However, many of the NW–SE-trending faults cut the top Draupne seismic surface ('Base Cretaceous') indicating that they were active until the very end of rifting and also accommodated minor extension during the immediate post-rift phase.

The structural elevation of the study area as a whole increases towards the northeast (Figs. 4 and 5c), although within the study area there is no significant decrease in the throw of the MSNFZ in the northeast (Fig. 6). The increase in structural elevation is most likely related to the influence of longer wavelength deformation associated with the Snorre Fault Zone to the northeast (Fig. 1). Over 1200 m of pre-rift strata have been eroded off the Snorre footwall structure in response to uplift during rifting, with Triassic units sub-cropping beneath the 'Base Cretaceous' (Hollander, 1987; Yielding, 1990; Dahl and Solli, 1993).

4.2. Fault displacement characteristics

A fault displacement–distance (D–d) profile was generated for the pre-rift top Statfjord Formation by systematically recording the vertical component of displacement (throw) in milliseconds (ms) two-way-travel-time (TWT), at intervals of 120 m along the length of the fault zone (Fig. 6). The seismic data have not been depth converted. Therefore, true displacement cannot accurately be measured because the dip of the fault is uncertain; consequently, throw is used as a proxy for displacement. The D–d profile was constructed for the top Statfjord horizon because it is generally free from footwall crestal erosion and hence footwall and hanging wall cut-offs can be determined with a good deal of accuracy (±5 ms TWT). In contrast, the top Brent Group and top Dunlin Group have been eroded along the footwall crest of the fault zone, especially in the northeast, and consequently the footwall cut-offs cannot always be determined accurately (e.g. Fig. 5b). The throw values recorded for the offset top Statfjord Formation do not necessarily represent the maximum throw on the MSNFZ, because it is unclear whether the offset bedding surface intersects the centre of the fault. The D–d profile has been modified in the region where three footwall faults terminate against the MSNFZ (labelled 'fault intersection region' in Fig. 6). Movement on these younger, intersecting faults has produced additional displacement, unrelated to that directly associated with the MSNFZ.

The D–d profile can be divided into three main geometrical (fault) segments, namely Murchison Fault segment (MS), Jog Fault (JF) and Statfjord North Fault segment (SNS) (Fig. 6). The Murchison Fault segment has a length of 15 km from the edge of the study area in the southwest to its tip, and a maximum throw of 450 ms TWT (c. 710 m) (Fig. 6a). The Statfjord North Fault segment has a length of 11 km from the edge of the study area in the northeast to its

tip, and a maximum throw of 380 ms TWT (c. 600 m) (Fig. 6a). The Murchison and Statfjord North Fault segments both exhibit multiple displacement minima (as labelled in Fig. 6a) along their lengths, separated by local displacement maxima (Fig. 6a). The distance between successive displacement minima (or maxima) varies from <1 to 2.5 km, with the difference in displacement between minima and maxima generally <100 ms TWT (c. 160 m). Towards the centre of the MSNFZ (within the study area), the three fault segments (i.e. MS, JF and SNS) overlap producing a zone of more complex throw distribution (Fig. 6). The tips of the Murchison and Statfjord North Fault segments (tip of MS and tip of SNS; Fig. 6) represent the continuation of these faults beyond the branch point with the Jog Fault, and show an abrupt decrease in throw (Fig. 6a). For example, throw on the Murchison Fault segment decreases from 200 ms TWT (c. 315 m) to 50 ms TWT (c. 80 m) across the branch point. The tip of the Murchison Fault segment has a length of 2 km (northeast of the branch point) and a displacement that decreases from 50 ms TWT (c. 80 m) at the branch point, to zero at the tip in the northeast (Fig. 6). The tip of the Statfjord North Fault segment has a length of 1 km and a steep displacement gradient that decreases from 210 ms TWT (c. 330 m) at the branch point, to zero at the tip in the southwest. The Jog Fault has a length of 2 km and a displacement that decreases from 220 ms TWT (c. 350 m) at its western end to 130 ms TWT (c. 205 m) at its eastern end. When the throw on these three overlapping faults are summed, the resultant values form a relatively smooth transition between the Murchison and Statfjord North Fault segments.

4.3. Insights into the fault zone evolution from analysis of structural characteristics

Analysis of the structural geometry and D–d profile suggest that the MSNFZ originally consisted of two individual fault segments, the Murchison and Statfjord North Fault segments, that subsequently became hard-linked by the Jog Fault (Fig. 4). This is indicated by: (1) the distinct jog or bend in the Murchison–Statfjord North fault trace; (2) the southwesterly dip of the beds in the footwall and hanging wall of the Jog Fault (as opposed to the more common northwesterly dip), preserving the dip in a precursor relay ramp; and (3) the abrupt decrease in throw from the Murchison and Statfjord North Fault segments to their tips, across the branch point with the Jog Fault, suggesting abandonment of the fault tips as the Jog Fault hard-linked the Murchison and Statfjord North Fault segments. Following hard-linkage, the tip of the Statfjord North Fault segment passively subsided in the hanging wall of the linked fault zone, whilst the tip of the Murchison Fault segment was passively uplifted. The summed D–d profile in the zone of fault overlap (i.e. where MS, JF and SNS overlap) does not exhibit a maximum displacement value for the fault zone. In fact, a displacement low is preserved at the linkage site that has not been lost by increased displacement following linkage as suggested by previous studies (Peacock and Sanderson, 1991; Cartwright et al., 1995; Dawers and Anders, 1995; Willemse et al., 1996). This implies that the linkage occurred late in the rift phase and hence is less advanced. However, the displacement deficit may also be due to other factors, such as overlap and separation of the two fault segments.

Displacement maxima and minima have been used in other studies to infer the centres and tips, respectively, of individual fault strands that have linked to form a single, through going fault segment (Peacock and Sanderson, 1991; Anders and Schlische, 1994). Applying these ideas to the D–d profile for the MSNFZ suggests that the Statfjord North Fault segment is composed of at least five main linked fault strands separated by displacement minima that preserve the location of remnant fault strand boundaries (black dots in Fig. 6a). The D–d profile for the Murchison Fault segment has numerous displacement minima suggesting that the fault segment is composed of multiple, linked precursor fault strands (Fig. 6a). In some instances, intra-basin structural highs within the hanging wall (labelled H; Fig. 6b) coincide with the location of displacement minima, providing further evidence that some of these displacement minima represented significant (relatively long-lived) fault strand boundaries.

5. Syn-rift stratigraphic evolution: implications for the timing of fault growth and linkage

The temporal and spatial evolution of major normal fault zones is accompanied by changes in basin topography and the location and generation of accommodation space (Schlische and Anders, 1996). Therefore, the architecture and distribution of the coeval stratigraphy has the potential to provide a record of tectonic evolution. The syn-rift stratigraphy deposited during the growth and linkage of the MSNFZ may therefore provide a record of the evolution of the fault zone by reflecting variations in subsidence during deposition. The aim of this section is to analyse the Late Jurassic syn-rift within the hanging wall of the MSNFZ, in order to place constraints on the evolving fault structure. The approach has essentially been threefold, involving: (1) analysis of thickness variations within major, seismically-defined syn-rift units; (2) locating intra-basin topographic highs; and (3) analysis of the spatial distribution of internal syn-rift seismic units.

Thickness (isochron) maps in milliseconds (TWT), were generated for the two main seismic divisions (Seismic Units 1 and 2) of the Late Jurassic syn-rift, which correspond to the Heather and Draupne Formations (Fig. 7a and b). Spatial variations in sediment thickness are used as a proxy for spatial variations in subsidence, and *not* as a direct measure of subsidence. This is because the quantitative link between preserved stratal thickness and actual subsidence depends

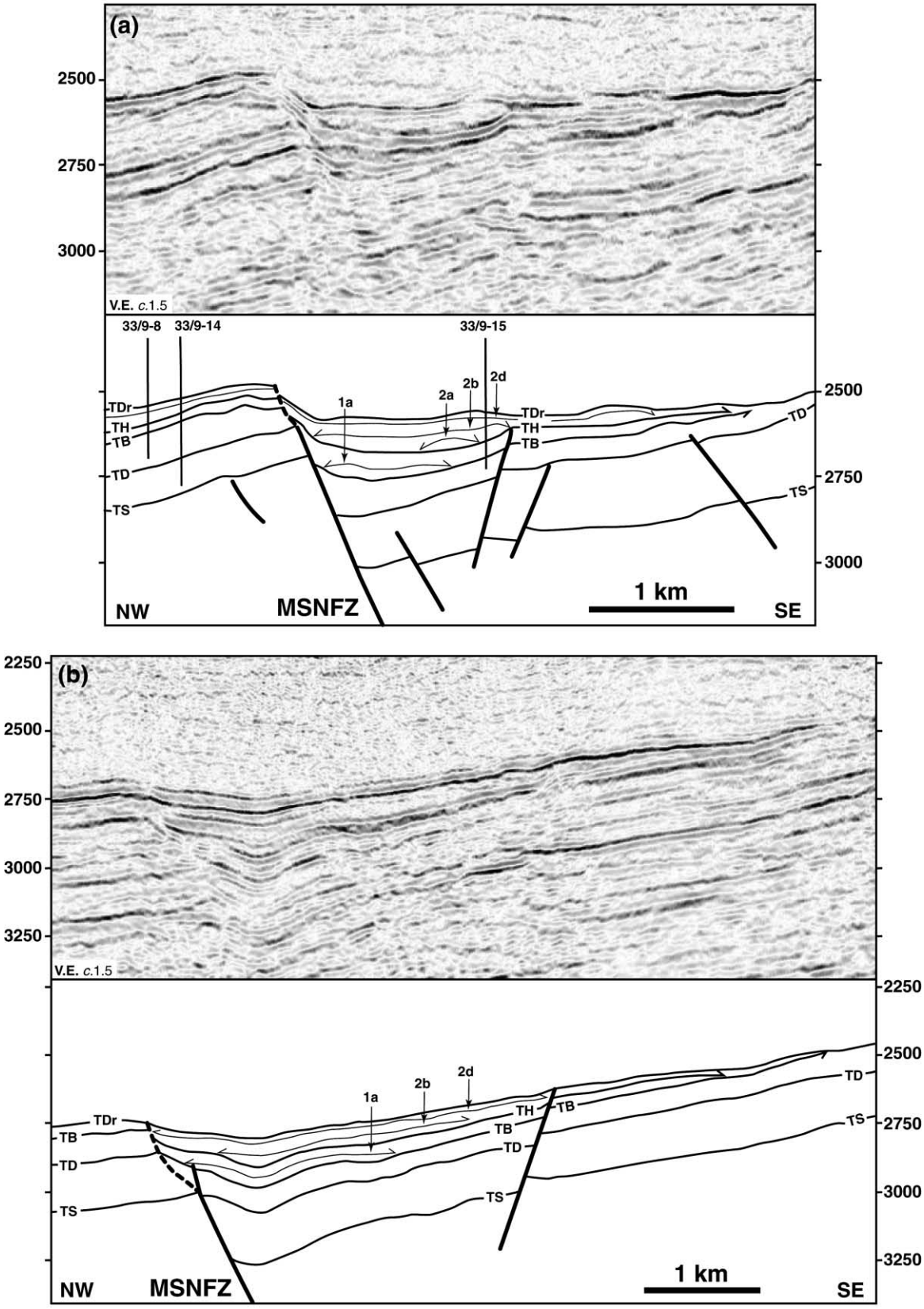

Fig. 5. (a) and (b) Seismic sections perpendicular to the Murchison–Statfjord North Fault Zone; (c) and (d) parallel to the fault, within the hanging wall of the Murchison and the Statfjord North Fault segment respectively. Vertical scale in ms TWT. V.E. = vertical exaggeration; TS = top Statfjord Formation; TD = top Dunlin Group; TB = top Brent Group; TH = top Heather Formation; TDr = top Draupne Formation ('Base Cretaceous'). Location of the lines is shown in Fig. 4a.

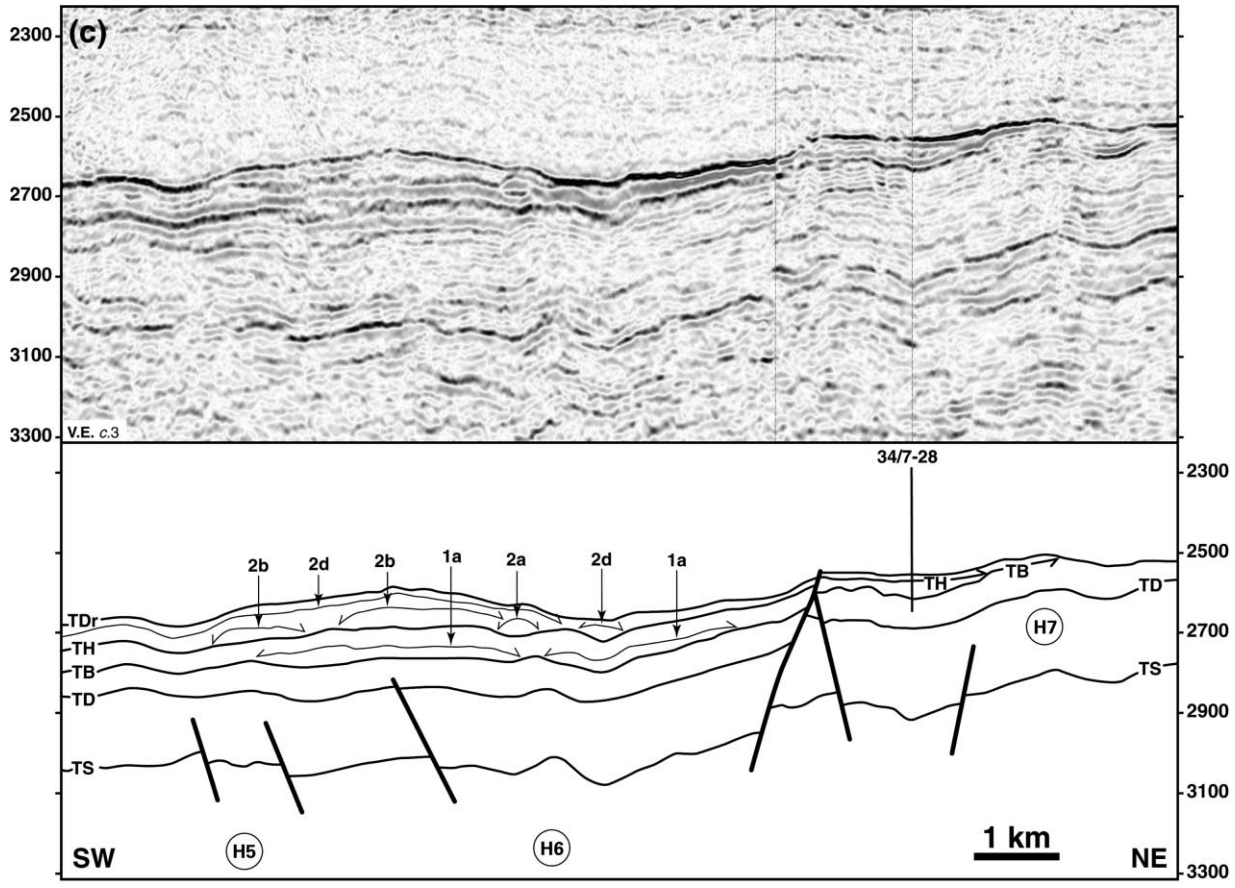

Fig. 5. (*continued*)

on a number of variables such as water depth, sedimentation rate/regime and compaction, all of which are difficult to quantify and are liable to vary through time. Therefore, we have taken a pragmatic approach by using bulk, preserved sediment thickness as a first order proxy for subsidence.

Previous studies of normal fault zones suggest that fault strand boundaries commonly represent regions of displacement deficit, expressed as hanging wall highs or transverse anticlines (Gawthorpe and Hurst, 1993; Gawthorpe et al., 1994; Anders and Schlische, 1994; Schlische, 1995; Schlische and Anders, 1996). After the fault strands have hard-linked and the boundary or high is ruptured, it passively subsides as part of the hanging wall. Consequently, the recognition of intra-basin topographic highs enables us to determine the location at which fault strands have linked together. Onlap of syn-rift seismic reflectors onto intra-basin highs gives an indication of the time period during which the high was a positive topographic feature and hence marked a boundary between individual fault strands.

There are several intra-syn-rift seismic reflectors that define spatially restricted seismic units (Fig. 5). During the deposition of a significant portion of the syn-rift stratigraphy, the half graben (controlled by the MSNFZ) would have been a fully marine domain, generally having deep water conditions, as indicated by the mudstone-dominated nature of much of the syn-rift stratigraphy; in particular the Heather Formation and lower part of the Draupne Formation (Nøttvedt et al., 2000). Under deepwater conditions the stratal geometries of the syn-rift seismic units are likely to reflect variations in the basin floor, fault-controlled topography, related to fault evolution rather than fluctuations in sediment supply or eustatic controls (Underhill, 1991). This is because deeper water sediments will preferentially be deposited, by gravity-driven processes, in topographic lows.

5.1. Characteristics of Seismic Unit 1 (Heather Formation)

5.1.1. Thickness data

The isochron map of Seismic Unit 1 (that corresponds to the Heather Formation) shows considerable variation within the immediate hanging wall of the MSNFZ. Six main isochron thicks (i.e. regions of maximum thickness in ms TWT) are observed (labelled D1–D6; Fig. 7a), trending parallel to the MSNFZ and separated by thinner regions. These isochron thicks are each <4 km in length (strike-parallel), <2 km in width, and have a maximum thickness of <100 ms TWT ($<$c. 160 m). Isochron thicks D1, D2 and D6 all occur immediately adjacent to the trace of the MSNFZ, whereas D3–D5 are situated up to 1 km away from the fault, with strata thinning towards the fault (Fig.

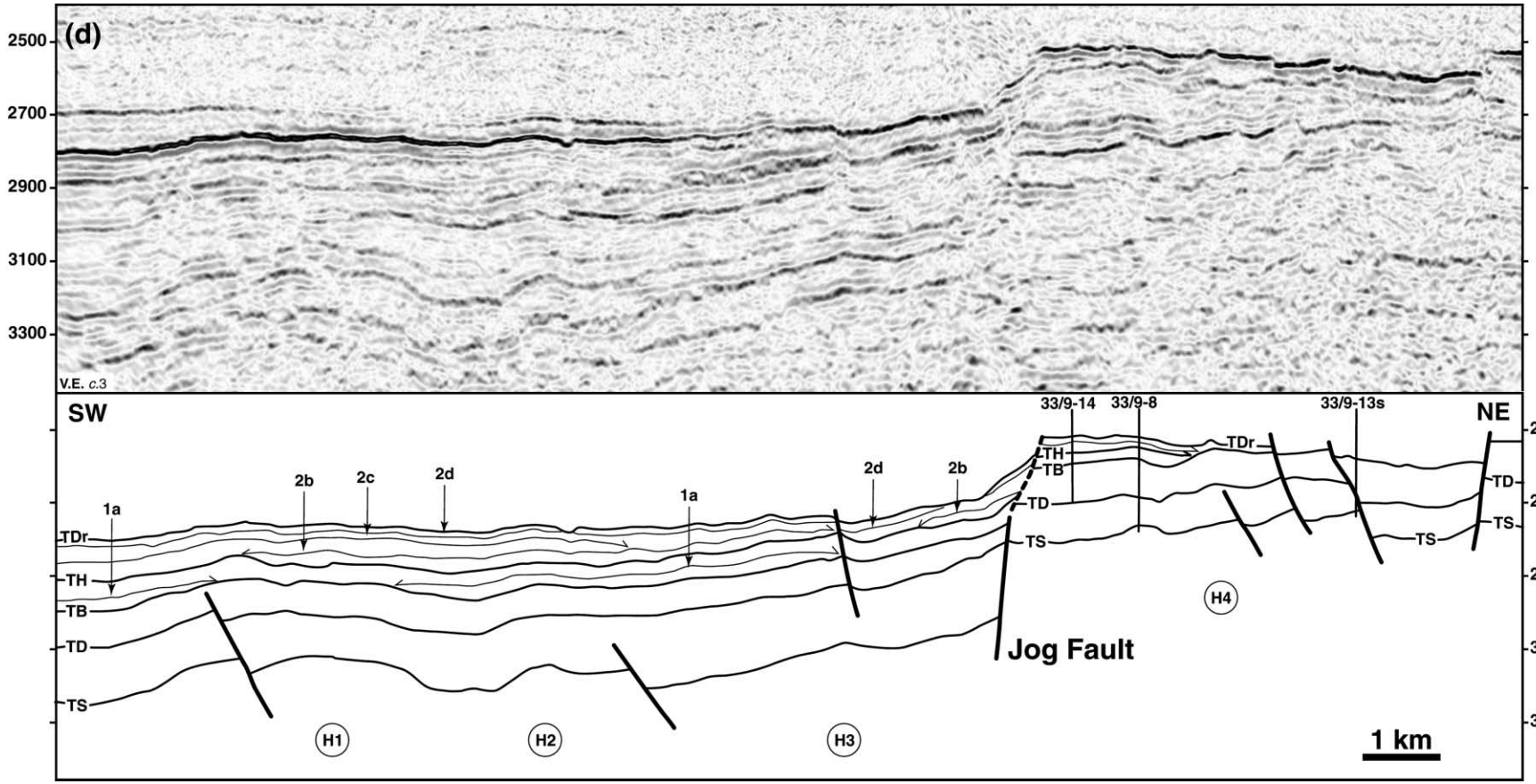

Fig. 5. (*continued*)

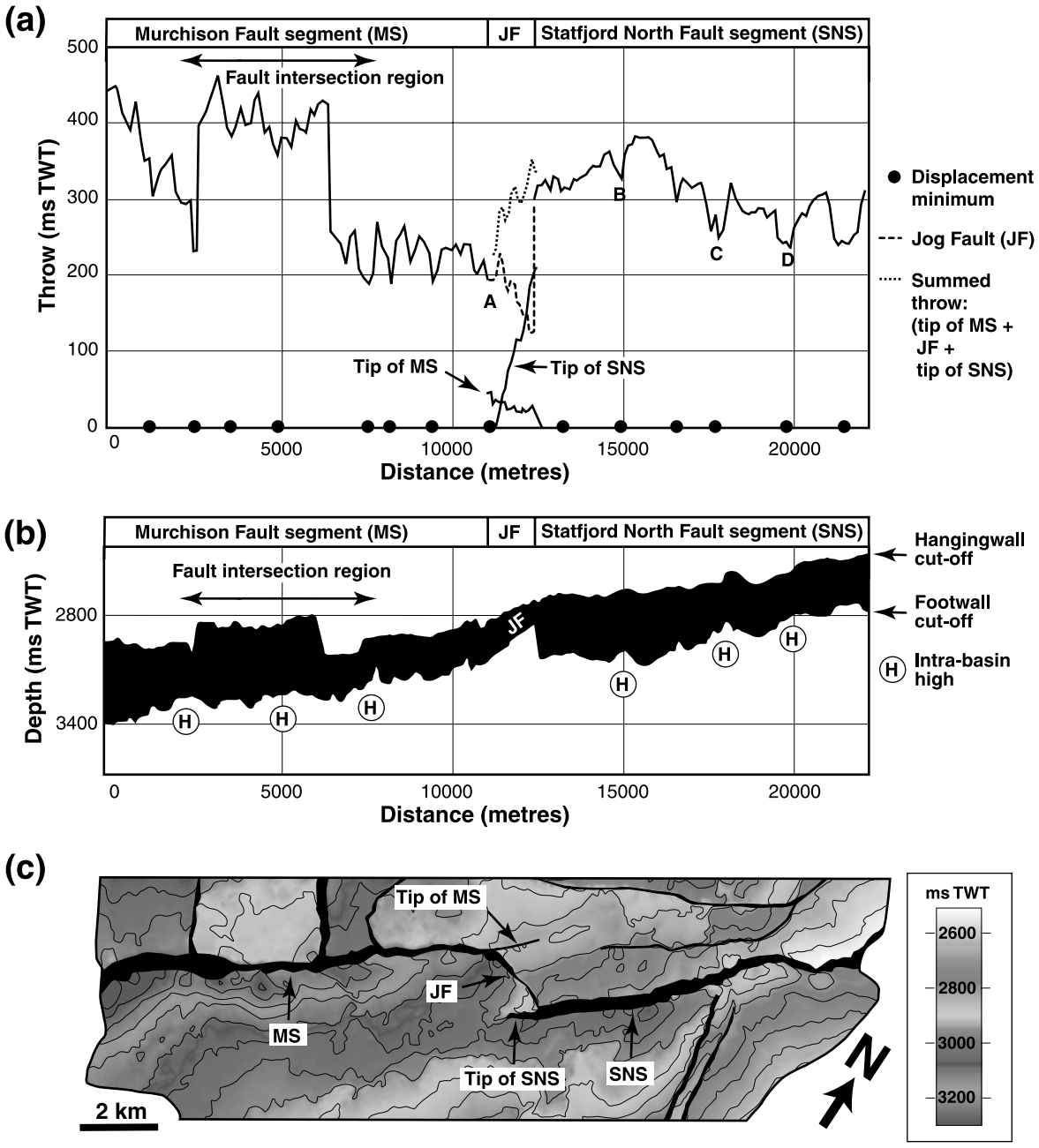

Fig. 6. (a) Fault *D–d* profile (vertical throw) generated for the top Statfjord Formation. MS = Murchison Fault segment; JF = Jog Fault; SNS = Statfjord North Fault segment; A–D refer to the location of displacement minima shown in Fig. 7. (b) Profile of the fault plane, showing hanging wall and footwall cut-off lines in ms TWT. (c) Map view of the fault trace, as shown in Fig. 4.

7a). Within the relay zone (i.e. current hanging wall and footwall of the Jog Fault), Seismic Unit 1 is significantly thinner than in the hanging wall of the Murchison and Statfjord North Fault segments (Fig. 7a). The thickness, however, gradually increases away from the Jog Fault towards the southwest, into the hanging wall of the Murchison Fault segment (Fault 3), whereas it increases abruptly to the east across the Statfjord North Fault segment (Fault 4). In general, the footwall of the MSNFZ contains a relatively thin, but even, thickness of Seismic Unit 1 that, for the purposes of this study, has not been investigated.

5.1.2. Intra-basin highs and onlap patterns

On strike-parallel seismic sections within the hanging wall of the MSNFZ, several intra-basin topographic highs (anticlines) can be identified (labelled H1–H7; Fig. 5c and d). There are three highs in the hanging wall of the Murchison Fault segment (H1–H3), one high in the footwall of the Jog Fault (H4), and three highs in the hanging wall of the Statfjord North Fault segment (H5–H7). An intra-Heather seismic reflector (Surface 1a) onlaps onto several of these intra-basin highs (e.g. H1 and H3–H7; Fig. 5c and d). Seismic Unit 1 also onlaps the eroded footwall crest of the

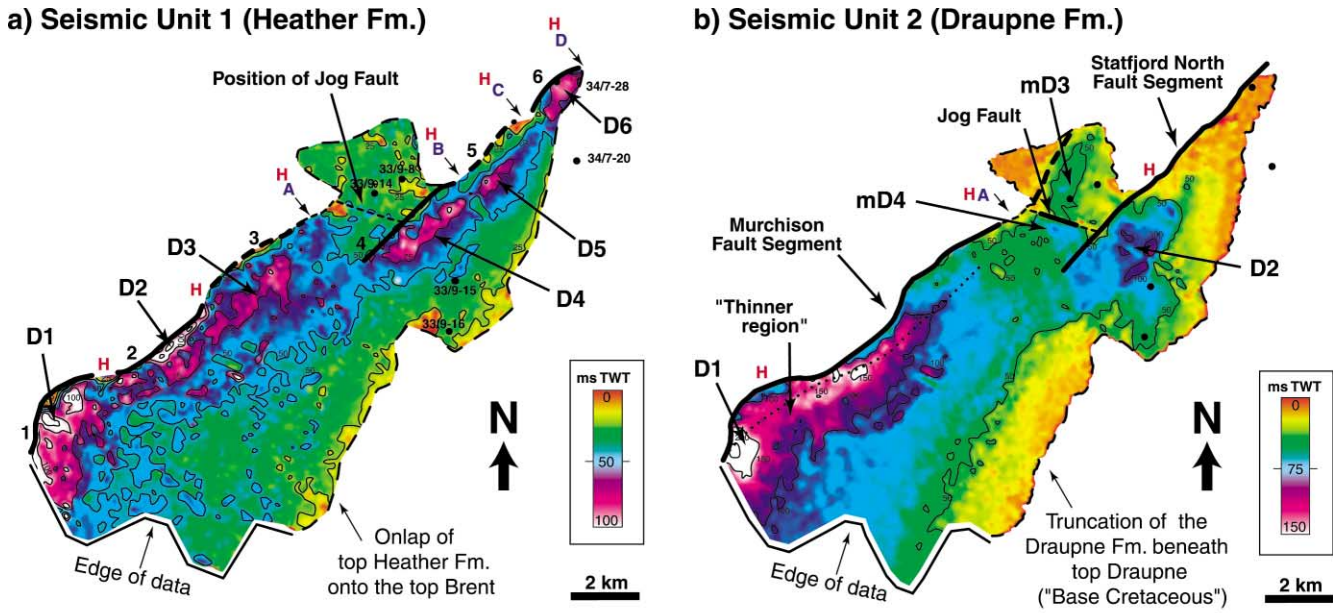

Fig. 7. Isochron (thickness) maps (ms TWT). Solid fault traces indicate a surface breaking fault (that controlled deposition), whilst the thick dashed fault trace represents a blind fault. The thin fault trace marks the MSNFZ trace as observed at the present day. A–D refer to the location of fault displacement minima (as shown in Fig. 6a) that correspond to fault strand boundaries. H refers to the location of intra-basin highs observed on fault parallel seismic lines (Fig. 5c and d). (a) Seismic Unit 1, corresponding to the Heather Formation (mid-Bathonian to mid-Oxfordian); D1–D6 refer to the major depocentres; 1–6 refer to the main fault strands (thick black lines) controlling the location of the depocentres, where 1–3 represent the pre-linked Murchison Fault segment and 4–6 represent the pre-linked Statfjord North Fault segment. (b) Seismic Unit 2, corresponding to the Draupne Formation (Late Oxfordian to mid-Ryazanian); D1 and D2 refer to the major depocentres; mD3 and mD4 refer to minor depocentres; the dotted line follows the axis of depocentre D1.

MSNFZ along much of its length, and is commonly deposited above the eroded tip of the fault, situated at the base of the eroded footwall scoop (e.g. Fig. 5b).

5.1.3. Spatial distribution of sub-units within Seismic Unit 1

On the basis of an intra-Heather seismic reflector (Surface 1a), Seismic Unit 1 (i.e. the Heather Formation) can be divided into two sub-units (Figs. 5 and 8a). Biostratigraphic dating indicates that the Heather Formation extends from the mid-Bathonian to the mid-Oxfordian, an interval of c. 10 myr based on the timescale of Gradstein et al. (1995). The initial seismic unit (Seismic Unit 1a), bounded above by Surface 1a, has a limited areal extent, occurring in a strip that is <2 km in width, within the immediate hanging wall of the MSNFZ (Fig. 8a). Seismic Unit 1a occurs in three separate regions in the hanging wall of the Statfjord North Fault segment and a single axial strip, of varying thickness, in the hanging wall of the Murchison Fault segment (Fig. 8a).

5.2. Insights into the fault zone evolution from analysis of Seismic Unit 1

Assuming that stratal thickness provides a qualitative record of subsidence, isochron thicks can be inferred to depict depocentres (i.e. regions of greatest subsidence). Therefore, the isochron map for Seismic Unit 1 indicates that there were six main, long-lived depocentres (D1–D6) that exerted the primary control on the observed seismic stratigraphic characteristics, and, hence, depositon of the Heather Formation (Fig. 7a). The isochron thicks (i.e. depocentres) are separated by thinner regions that correspond to intra-basin structural highs (labelled H; Fig. 7a) identified on seismic sections (Fig. 5c and d). The six depocentres are interpreted to have been controlled by six individual fault strands (labelled 1–6; Fig. 7a), with the strand boundaries, regions of displacement deficit, marked by intra-basin topographic highs (Fig. 7a). Several of the intra-basin highs are onlapped by Surface 1a, demonstrating that they had a positive topographic expression during deposition, with Seismic Unit 1a absent or below seismic resolution above the highs (Fig. 5c and d). The individual fault strands are interpreted to have exerted the primary control on subsidence variations and basin floor topography during the deposition of Seismic Unit 1. While differential compaction of syn-rift sediments could produce comparable stratal geometries and thickness patterns, the folding that defines the depocentres and marks the intra-basin structural highs also affects the pre-rift stratigraphy, favouring a structural origin to these features. The onlap of Surface 1a onto, and the absence of Seismic Unit 1a from above, some of the intra-basin topographic highs (Fig. 5c and d) indicates that relatively little deposition initially occurred above them, because they were fault-controlled highs during early deposition; although this may also be a consequence of a low sediment supply. However, the half-graben does not appear to be significantly ‘under-filled’ (Fig. 5), and, therefore, we assume that sufficient sediment was deposited, during rifting, to at least fill the fault-generated

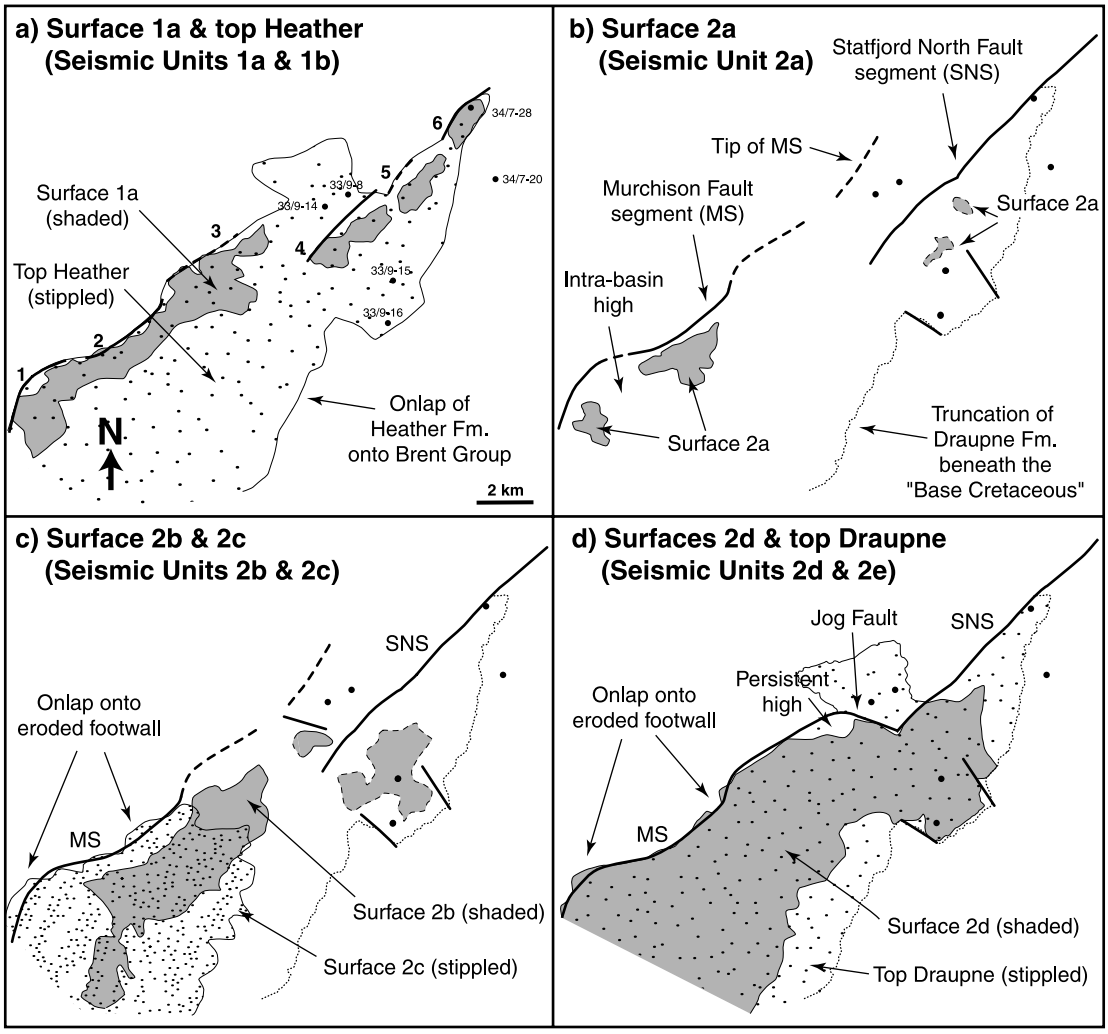

Fig. 8. Maps showing the extent of seismic surfaces/seismic units within (a) Seismic Unit 1; and (b)–(d) Seismic Unit 2. 1–6 refer to the fault strands controlling the location of depocentres (as for Fig. 7). MS = Murchison Fault segment; SNS = Statfjord North Fault segment.

basin floor topography, such that the depositional surface was continually changing in unison with the evolving fault structure.

The depocentres in the hanging walls of Faults 1, 2 and 6 are located directly against the fault trace, suggesting that the controlling fault strands were surface breaking faults during much of the deposition of Seismic Unit 1, with the greatest subsidence in the immediate hanging wall of the faults. However, the depocentres in the hanging walls of Faults 3, 4 and 5 are situated up to 1 km away from the fault trace, suggesting that the controlling fault segments were blind, upward propagating faults during much of the deposition of Seismic Unit 1. This was expressed at the surface as fault propagation folds, with the greatest subsidence occurring to the east (basinward) of the fault trace (Withjack et al., 1990; Gawthorpe et al., 1997; Hardy and McClay, 1999) (Fig. 7a). However, these observations may also reflect the amount of onlap onto the eroded footwall crest and overstepping of the eroded fault tip (e.g. compare Fig. 5a and b).

Deposition of the mudstone-dominated Heather Formation was focused (by gravity-controlled sediment transport) into the depocentres (structurally-controlled topographic lows), with strata onlapping the margins of the local depocentres, as indicated by the onlap pattern of Surface 1a and its areal extent (Figs. 5c and d and 8a). Seismic Unit 1 is thinner in the hanging wall and footwall of the Jog Fault than in the hanging walls of the Murchison and Statfjord North Fault segments (Fig. 7a). This implies that the region around the Jog Fault had a greater topographic relief and, hence, less sediment accumulated by comparison to the main depocentres. Furthermore, there is a fairly gradual thinning of Seismic Unit 1 from the hanging wall of the Murchison Fault segment, through the hanging wall of Jog Fault and into the footwall of the Statfjord North Fault segment (Fig. 7a). This suggests that during the deposition of the Heather Formation, a relay ramp existed between the two main fault segments (Murchison and Statfjord North Fault segments) which, at this time, were themselves composed of individual fault strands.

The deposition of Seismic Unit 1 above the eroded fault tip, and onlapping the eroded footwall crest of the MSNFZ, indicates that a considerable amount of footwall degradation occurred early, during or prior to the deposition of the seismic unit. The fault does not appear to have propagated up through Seismic Unit 1 during continued subsidence (Fig. 5b).

5.3. Characteristics of Seismic Unit 2 (Draupne Formation)

5.3.1. Thickness data

The isochron map of Seismic Unit 2 (that corresponds to the Draupne Formation) shows less thickness variability in the immediate hanging wall of the MSNFZ than that of Seismic Unit 1 (Fig. 7b). Two major isochron thicks (D1 and D2; Fig. 7b) and two minor isochron thicks (mD3 and mD4; Fig. 7b) can be observed in the hanging wall and footwall of the MSNFZ (Fig. 7b). In the hanging wall of the Murchison Fault segment, one major isochron thick (D1) is evident, 9 km in length, <3 km in width, with a maximum thickness of 200 ms TWT (c. 395 m). The thickness of D1 is greatest in the southwest and overall decreases along-strike towards the northeast, although in detail there is some variability (Fig. 7b). Along the length of its axis (shown by the dotted line; Fig. 7b), D1 is commonly situated up to 1 km from the fault trace, although where thickness is greatest it is situated immediately adjacent to the fault trace. In the hanging wall of the Murchison Fault segment, beyond the branch point with the Jog Fault, one minor isochron thick (mD3) is evident, 2 km in length, <1 km in width, with a maximum thickness c. 50 ms TWT (c. 80 m). The axis of mD3 is situated c. 500 m from the fault trace. In the hanging wall of the Statfjord North Fault segment, one major isochron thick (D2) is evident, 4 km in length, 2 km in width, with a maximum thickness of >100 ms TWT (>160 m). Along-strike to the northeast of D2, Seismic Unit 2 decreases in thickness considerably to <25 ms TWT (<c. 40 m) (Fig. 7b). In the hanging wall of the Jog Fault, one minor isochron thick (mD4) is evident, <1 km in length and width, with a maximum thickness c. 50 ms TWT (c. 80 m).

5.3.2. Intra-basin highs and onlap patterns

Intra-Draupne seismic reflectors can be observed to onlap the top Heather reflector in several places (Fig. 5c and d). A number of these onlap terminations corresponds with the location of intra-basin highs (e.g. H1, H3 and H4; Fig. 5d) that fold the pre-rift strata and also Seismic Unit 1 (i.e. the Heather Formation). Seismic Unit 2 also onlaps the eroded footwall crest of the MSNFZ along much of its length (e.g. Fig. 5b).

5.3.3. Spatial distribution of sub-units within Seismic Unit 2

On the basis of four intra-Draupne seismic reflectors (Surfaces 2a–2d), Seismic Unit 2 is divided into five sub-units (Seismic Units 2a–2e) that are often restricted to local regions in the hanging wall of the MSNFZ (Fig. 8b–d). However, the surfaces generally cover a progressively larger area of the half-graben through time (Figs. 5 and 8b–d). The age relationships between the various surfaces (seismic reflectors) are based on their relative stratigraphic positions within Seismic Unit 2, and by stratal terminations against the other surfaces.

The core data from well 33/9-15 enable Surface 2b to be biostratigraphically constrained to top mid-Volgian age, and also indicate that Surface 2b is an hiatal surface of non-deposition that is coincident with a significant, mid-Volgian eustatic sea-level fall (Sahagian et al., 1996) (Fig. 3). The seismic units between the top Heather reflector and Surface 2b (i.e. Seismic Units 2a and 2b) extend from the mid-Oxfordian to mid-Volgian, an interval of c. 10.5 myr based on the timescale of Gradstein et al. (1995). The core data (well 33/9-15) indicate that Seismic Unit 2b is composed of an inter-bedded succession of turbidite sandstones and mudstone; bottom-seeking, relatively deep-water gravity deposits (Fig. 3). The Seismic Units between Surface 2b and the top Draupne reflector (i.e. Seismic Units 2c–2e) extend from the mid-Volgian to mid/late Ryazanian, an interval of c. 7 myr based on the timescale of Gradstein et al. (1995). The core data (well 33/9-15) indicate that Seismic Units 2d and 2e are composed of a progradational shoreface sandstone succession; a relatively shallow water deposit (Fig. 3). Seismic Unit 2c (bounded above by Surface 2c) is absent from the region encompassing well 33/9-15, only occurring down-dip in the southeastern part of the half-graben (Fig. 8).

5.4. Insights into the fault zone evolution from analysis of Seismic Unit 2

Assuming that isochron thicks depict regions of greatest subsidence (i.e. depocentres), the thickness map for Seismic Unit 2 (Draupne Formation) suggests that during its overall deposition, subsidence was less variable along-strike than that which occurred during the overall deposition of Seismic Unit 1 (Heather Formation), as a consequence of fault linkage. The thickness data for Seismic Unit 2 indicate that a fault configuration consisting of two main overlapping fault segments (the Murchison and Statfjord North segments) soft-linked by a relay ramp exerted the primary control on the deposition of Seismic Unit 2. This is because two main isochron thicks (D1 and D2) and, hence, depocentres are observed in the hanging walls of the Murchison and Statfjord North Fault segments (Fig. 7b). Along the Murchison Fault segment, Seismic Unit 2 thins considerably towards the Jog Fault (by >100 ms TWT; >c. 160 m) and there is only a minor depocentre in the hanging wall of the Jog Fault (Fig. 7b). This suggests that the Jog Fault hard-linked the two main fault segments (Murchison and Statfjord North) at a relatively late stage in the rift event, and there was not enough recurrent seismicity in the rift system for significant subsidence to occur in the area of linkage.

The more continuous depocentre in the hanging wall of the Murchison Fault segment suggests that the earlier co-linear fault strands, active during the deposition of Seismic Unit 1, had linked to form a longer fault segment (i.e. the Murchison Fault segment). Thus, the hanging of the Murchison Fault segment subsided as a single fault segment, with displacement decreasing northeastwards towards the fault tip. However, the thickness map for Seismic Unit 2 indicates that there is a 'thinner region' in the hanging wall of the Murchison Fault segment (as labelled in Fig. 7b), up to c. 50 ms TWT (c. 80 m) thinner than the regions to the northeast and southwest of it. This 'thinner region' corresponds to the intra-basin high that marked the boundary between Faults 1 and 2 during the deposition of Seismic Unit 1 (Fig. 7). Furthermore, within this 'thinner region', Surface 2b onlaps onto a topographic high (at top Heather level) produced by the folding of the pre-rift and Seismic Unit 1 (Fig. 5d). This implies that the structural high (fault strand boundary) persisted in this location during the depositon of the early part of Seismic Unit 2, at least up to Surface 2b. Thus, either Faults 1 and 2 linked during the deposition of the seismic unit, or the high was preserved after linkage and continued to affect deposition whilst it passively subsided in the hanging wall of the linked fault segment.

The thickness data from the hanging wall of the Statfjord North Fault segment do not enable any firm insights to be made into the evolution of this fault segment during the depositon of Seismic Unit 2. The thickness decrease against the northeastern part of the Statfjord North Fault segment does not correspond with a significant decrease in fault throw (Fig. 6). The northeastern region of the study area, however, does have the highest structural elevation (Fig. 4). This suggests that fault-controlled subsidence and the development of accommodation space in this northeastern region was suppressed and/or the deposited sediment was eroded, due to long-wavelength uplift that was linked to the development of adjacent fault zones, in particular Snorre to the northeast (Figs. 1 and 4), where it is suggested that over 1200 m of uplift has occurred (Hollander, 1987; Yielding, 1990; Dahl and Solli, 1993).

The intra-Draupne seismic surfaces have a progressively greater areal extent up-stratigraphy, suggesting that the evolving half-graben was becoming wider and subsiding more uniformly through time as a fault linkage progressed and the basin filled. It is important, however, to consider the significant variations in facies and depositional conditions that occur across Surface 2b, an hiatal surface coincident with a eustatic sea-level fall. Below Surface 2b, Seismic Units 2a and 2b are composed of bottom-seeking turbidities (Fig. 3), deposited in topographic lows, and, hence, the primary control on their architecture and distribution was fault-controlled subsidence. Above Surface 2b, however, deposition was also influenced by eustasy, with a significant relative sea-level fall occurring prior to or even during the deposition of Seismic Units 2c–2e. Consequently, it is difficult to determine the primary control on their architecture and distribution. Furthermore, it is known that a shoreface succession was prograding into the basin from the northeast during the deposition of Seismic Units 2d and 2e (Fig. 3), which could have resulted in greater deposition on the hanging wall dip-slope rather than in the depocentres in the immediate hanging wall of the fault zone.

6. Tectono-stratigraphic evolution of the Murchison–Statfjord North Fault Zone

The aim of this section is to integrate the structural and stratigraphic data presented in this paper, to constrain the temporal and spatial evolution of the northern 25 km length of the MSNFZ. The evolution has been divided into three main stages in which the fault configuration, depocentres and idealised displacement profile have been reconstructed (Fig. 9). The first stage corresponds to the deposition of Seismic Unit 1 (Heather Formation), whilst the second and third correspond to the deposition of Seismic Unit 2 (Draupne Formation).

6.1. Isolated fault strands

This stage represents fault development and deposition of Seismic Unit 1 (Heather Formation) from the mid-Bathonian to mid-Oxfordian, a time interval of c. 10 myr based on the timescale of Gradstein et al. (1995). Rifting initiated and the fault zone developed a configuration consisting of six main isolated fault strands, <4 km in length, with local depocentres in their hanging walls (Fig. 9a). This is interpreted to have been the primary structural configuration that controlled the architecture and spatial distribution of the mudstone-dominated Heather Formation. Deposition occurred by gravity-driven sediment transport processes, in structurally-controlled topographic lows. Previous studies of the northern North Sea syn-rift consider the Tarbert Formation, deposited during the latest Bajocian, to be the initial syn-rift deposit (Ravnås et al., 1997), something which cannot be proven by this study. If this is the case, however, the fault configuration described here is likely to have developed and persisted for up to c. 3 myr longer (i.e. for the initial c. 13 myr of rifting). Four of the isolated fault strands are interpreted to have broken surface early and, hence, strata thicken into the fault (Fig. 9a). The other two fault strands broke surface later, and for much of this early rift stage were blind, forming monoclines at the surface, with strata thickening into synclinal depocentres situated to the east of the buried fault trace. The fault strand boundaries (margins of the hanging wall depocentres) were marked by intra-basin topographic highs, a number of which were onlapped by Surface 1a (intra-Heather seismic reflector) which was preferentially deposited within the main fault-controlled depocentres (Figs. 5 and 8).

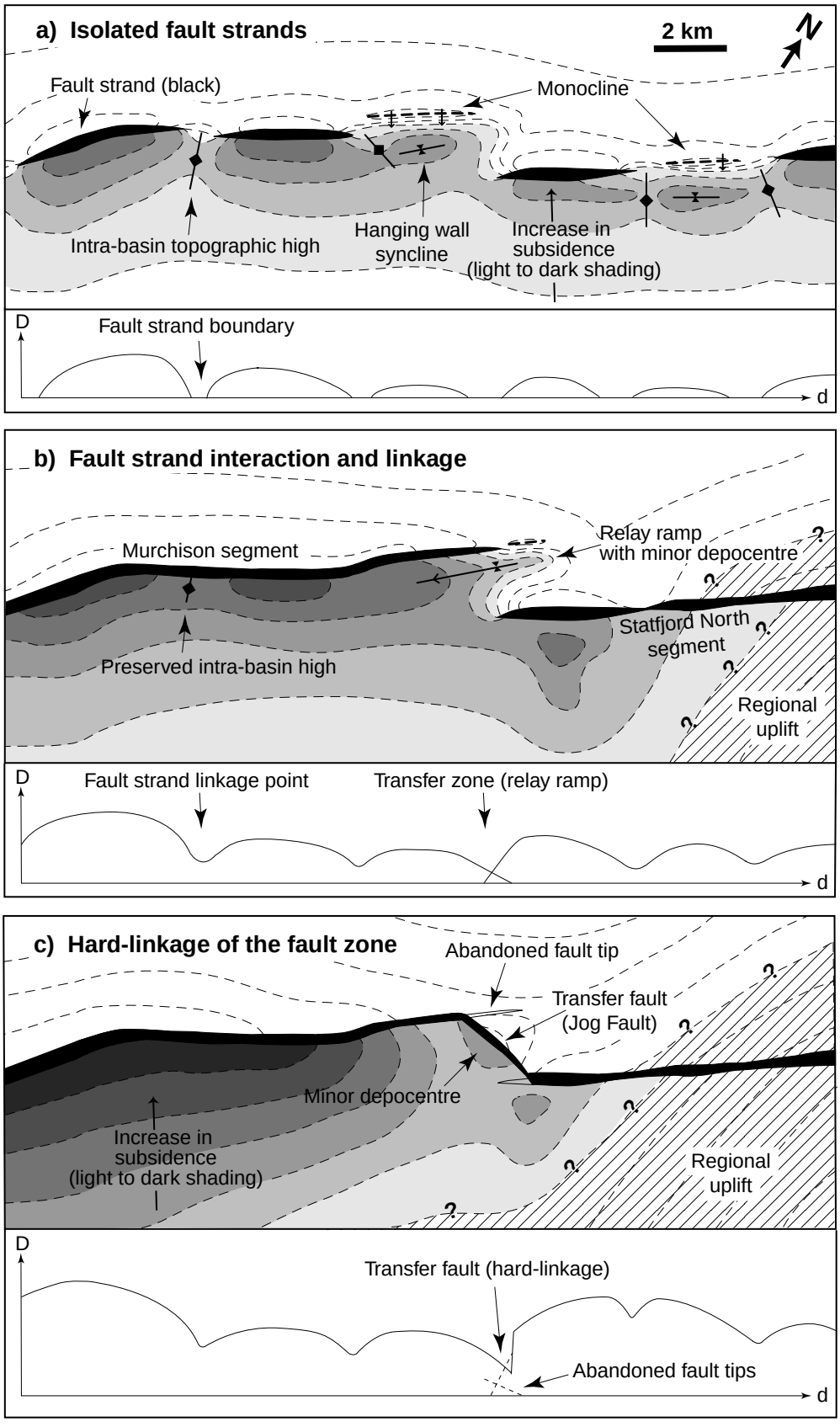

Fig. 9. Summary diagrams showing the three main stages in the evolution of the Murchison–Statfjord North Fault Zone, along with a reconstruction of the fault displacement–distance profile. The light to dark shading indicates an increase in subsidence. (a) Isolated fault strands; (b) co-linear strands link, producing two fault segments separated by a relay ramp; (c) hard-linkage, forming a single continuous fault trace, as observed at the present day.

6.2. Fault strand interaction and linkage

This stage represents fault development and the deposition of Seismic Unit 2 (Draupne Formation), during a phase of ongoing fault interaction and linkage, from the mid-Oxfordian to mid-Ryazanian, a time interval of c. 17.5 myr based on the timescale of Gradstein et al. (1995). By the onset of, or early during, this stage, the isolated, co-linear fault strands (that controlled the deposition of Seismic Unit 1) linked along-strike, such that the fault zone consisted of two main fault segments (Murchison and Statfjord North), each >9 km in length and separated by a relay ramp (Fig. 9b). On the basis of the displacement deficit within the relay zone (Fig. 6) and the relatively thin Seismic Unit 2 in the hanging wall of the Jog Fault (Fig. 7b), the relay ramp is interpreted to have been breached, and the fault segments hard-linked late in the rift phase.

Seismic Unit 2b (bounded above by Surface 2b) is composed of relatively deep water, gravity-driven turbidite deposits (Fig. 3) that are inferred to reflect the fault-controlled basin topography. Seismic Unit 2b occurs in the hanging wall of both the Murchison and Statfjord North Fault segments, with the distribution suggesting the presence of a single depocentre in the hanging wall of each fault segment (Fig. 8c). Surface 2b is top mid-Volgian in age and is coincident with a eustatic sea-level fall. Seismic Units 2d and 2e are situated above this surface, and are composed of a relatively shallow water, regressive shoreface succession (Fig. 3), the distribution of which may not only reflect basin topography. However, Surface 2d, that occurs within this shoreface succession, is distributed across a wide area of the half-graben (Fig. 8d), suggesting that the basin topography was less complex, due to a combination of: (1) more uniform subsidence along the hard-linked fault zone, with no fault strand/segment boundaries to inhibit earthquake rupture or structurally compartmentalise the basin; and (2) filling of accommodation space due to an increase in sediment supply following eustatic sea-level fall.

We suggest that a structural configuration consisting of two main fault segments separated by a relay ramp (Fig. 9b), was the primary control on the architecture and distribution of the stratigraphy from the late Oxfordian until at least the mid-Volgian eustatic sea-level fall, an interval of c. 10.5 myr based on the timescale of Gradstein et al. (1995). Therefore, the fault zone became hard-linked during the final c. 7 myr of rifting (late-Volgian to mid-Ryazanian), during which time a maximum of 200 ms TWT (c. 315 m) of throw accumulated on the Jog Fault that breached the relay ramp (Fig. 9c).

During this phase of fault strand interaction and linkage, the three previously isolated (Heather Formation) depocentres along the Murchison Fault segment 'merged' and began to subside as a single depocentre, once the controlling fault strands had linked to form a longer fault segment (Fig. 9b). However, a minor intra-basin high still persisted in the hanging wall of the Murchison Fault segment after fault strand linkage (Fig. 9b), and affected deposition of the early Draupne Formation (Seismic Unit 2b), with Surface 2b onlapping the high (Fig. 5d). Regional uplift in the footwall of the Inner Snorre Fault, to the northeast of the study area, resulted in uplift of both the hanging wall and footwall of the MSNFZ, especially the Statfjord North segment, in the northeast of the study area (Figs. 4 and 9b). As a result, only one depocentre (isochron thick) developed and/or was preserved in the hanging wall of this fault segment, and, consequently, it is not possible to determine the nature of fault strand linkage. The combination of a thin, even distribution of Seismic Unit 2, regional uplift and eustatic sea-level fall suggests that erosion and non-deposition occurred in the northeastern part of the study area (Fig. 9b and c). The relay ramp that separated the two main fault segments dipped towards the southwest. Surfaces 2b and c, deposited in the hanging wall of the Murchison Fault segment, onlapped towards the relay ramp (Figs. 5d and 8c) which represented a relative high (Fig. 9b). A minor depocentre is interpreted to have formed within the relay ramp due to the propagation of the tip of the Murchison Fault segment or a fault ahead of this (Fig. 9b). Hard-linkage of the fault zone, however, resulted in the abandonment of subsidence within this region. The stratigraphy in the hanging wall of the Jog Fault only records a relatively minor depocentre, suggesting that there was not enough recurrent seismicity in the rift system for significant subsidence to occur in this area, following hard-linkage.

Displacement minima on the D–d profile generated for the final disposition of displacement on the MSNFZ mark the linkage points of the precursor fault strands (Fig. 9c). Based on a structural analysis alone, approximately 14 precursor fault strands are identified (Fig. 6a). However, on the basis of thickness variations within Seismic Unit 1, it can be inferred that only six of these fault strands were important in controlling syn-rift stratal thickness. The length scale of each of these strands was <4 km (Fig. 9a). The fact that only six fault strands can be recognised in this study is perhaps a consequence of the resolution of the data used: i.e. seismic data with vertical resolution of 10–30 ms TWT (c. 15 to c. 50 m). At a higher resolution, it is possible that a record of all 14 precursor strands could be identified in the stratigraphy.

7. Discussion and implications

Structural data from normal fault zones, such as displacement–distance (D–d) profiles and fault trace geometry record the final disposition of displacement. Several previous studies have used D–d profiles to provide a qualitative insight into the growth history of normal faults (Gudmundsson, 1987a,b; Peacock and Sanderson, 1991; Dawers et al., 1993; Trudgill and Cartwright, 1994; Cartwright et al., 1996; Schlische et al., 1996; Cartwright and

Mansfield, 1998). Displacement minima along the *D–d* profile are interpreted to represent points at which isolated fault strands and segments linked during fault growth (Peacock and Sanderson, 1991; Cartwright et al., 1995; Cartwright and Mansfield, 1998). An interpretation of the pre-linkage history of a normal fault essentially relies on the assumption that displacement minima represent the location of fault linkages; an assumption that is reinforced if the minimum corresponds to an offset, overlap or change in strike of the fault trace (Peacock and Sanderson, 1991; Trudgill and Cartwright, 1994). The results from this study indicate that fault segments having a continuous and straight final trace geometry (e.g. the Murchison and Statfjord North fault segments) may exhibit numerous displacement irregularities (maxima and minima) when plotted on a *D–d* profile (Figs. 6 and 9). In the absence of geometric evidence from the fault trace, such as a bend or step, it is difficult to assess which of the multiple displacement minima are of significance and mark the linkage point between depocentre-controlling fault strands. For example, if all of the displacement minima along the Murchison–Statfjord North Fault Zone represent fault strand linkage points, then the fault zone formed through the linkage of at least 14 individual strands (Fig. 6a). However, analysis of syn-rift thickness variations reveals that only six individual fault strands had a significant control on the preserved stratigraphy and basin configuration during the initial c. 13 myr of rifting (Figs. 6a, 7a and 9). It is apparent that structural data alone do not allow a detailed insight to be made into the temporal or spatial evolution of a normal fault zone. Temporal and spatial patterns of fault growth and linkage can only be determined and constrained using stratigraphic information (e.g. thickness variations, stratal architecture and distribution) integrated with biostratigraphy or other dating techniques.

Numerical modelling studies of normal fault growth predict that a population of normal faults develop through a number of distinct stages during rifting (Cowie et al., 1995; Cowie, 1998; Gupta et al., 1998): (1) a nucleation stage of many isolated fault segments; (2) a stage in which optimally located faults, with respect to neighbouring structures, experience enhanced growth, with fault linkages occurring; and (3) a linkage stage in which deformation is localised onto a few through-going faults. These models predict the patterns of faulting produced as rifting progresses, but are unable to place any temporal constraints on the time interval over which distinct fault patterns exist and influence stratigraphic architecture and distribution. This study confirms the basic hypotheses for the growth and linkage of normal faults. In addition, the results from this study of the MSNFZ enable temporal constraints to be placed on the evolution of this long-lived, major basin-bounding fault zone during c. 30.5 myr of Late Jurassic rifting in the northern North Sea. The results suggest that: (1) following the initiation of rifting, isolated fault strands ($<$4 km in length) developed and exerted the primary control on basin structuration (e.g. location and size of depocentre) and stratigraphy during a time interval of up to c. 13 myr; and (2) the isolated fault strands progressively linked along-strike forming a single through-going fault by the end of rifting; a further time interval of up to c. 17.5 myr However, it was only during the last c. 7 myr of rifting that the fault zone hard-linked to form the single fault trace that is observed at the present day.

The comparable study of Dawers and Underhill (2000) investigated the evolution of the Statfjord East Fault Array, adjacent to the Murchison–Statfjord North Fault Zone (Fig. 1). They suggested that after rift initiation the deposition of the Heather and Draupne Formations occurred during a phase of ongoing linkage of fault segments. Lateral growth of the Statfjord East Fault Array by linkage is interpreted to have been on the order of 5–10 km in c. 20 myr It is suggested, in this paper, that following the 'initiation' phase of isolated fault strands, it took up to an additional c. 17.5 myr of ongoing linkage for the 25 km long north-eastern portion of the Murchison–Statfjord North Fault Zone to become a linked single fault structure. These time constraints are comparable, and suggest that faults within this region took on the order of 17–20 myr to evolve from isolated fault segments or strands to a single fault structure. It is probable that these timescales are similar, because the Murchison–Statfjord North Fault Zone and Statfjord East Fault Array are within the same rift regime and the faults have propagated through the same pre-rift lithologies.

8. Conclusions

Integrated analysis of the structure and stratigraphy of the Murchison–Statfjord North Fault Zone and adjacent syn-rift stratigraphy has demonstrated that the single, continuous through-going trace of the fault zone has developed through the propagation, interaction and linkage of originally isolated fault strands and segments. The evolution of the fault zone can be divided into three distinct stages. (1) During the initial c. 13 myr of rifting, the fault zone developed a structural configuration consisting of isolated fault strands, $<$4 km in length, with distinct local depocentres in their hanging walls that controlled the architecture and distribution of the Heather Formation (and probably the Tarbert Formation also). The fault strands and depocentres were separated by intra-basin topographic highs that marked fault strand boundaries. (2) c. 13 myr after rift initiation, the isolated fault strands had linked along-strike producing two $>$9 km long fault segments separated by a 2 km wide relay ramp; a structural configuration that exerted the primary control on the architecture and distribution of the Draupne Formation for at least a further c. 10.5 myr of rifting. (3) It was only during the final c. 7 myr of rifting that the two fault segments hard-linked to produce a single, continuous fault trace, as observed at the present day. The hard-linkage occurred

late in the rift event and the Draupne Formation essentially preserves the pre-linkage structure.

In order to place temporal constraints on the spatial patterns of fault evolution, this study suggests that it is necessary to integrate both structural data from the fault zone and stratigraphic data from the adjacent syn-rift. Analysis of sediment thickness variations, together with the architecture and distribution of syn-rift strata, tied to biostratigraphy, allow temporal constraints to be placed on depositional patterns produced by specific fault configurations. For example, based on a structural analysis alone, approximately 14 precursor fault strands are identified. However, on the basis of stratigraphic data it can be inferred that only six of these strands were important in controlling stratal architecture and distribution.

The results from this study have implications for the timing of normal fault evolution; in particular, the time scales over which specific fault patterns develop and exert a fundamental control on the syn-rift stratigraphy. This may help to further constrain models of fault evolution.

Acknowledgements

The authors gratefully acknowledge financial support from NERC (studentship GT/04/97/196/ES to MJY) and Saga Petroleum (now Norsk Hydro). Saga Petroleum are also acknowledged for providing access to the dataset. We acknowledge support from Schlumberger (GeoFrame seismic interpretation software) and Gocad (3D visualisation software). This work benefited from discussions with Terje Hellem, Jez Averty, Mike Whitaker, John Underhill, Ian Sharp, Emma Finch and Aileen McLeod. Nance Dawers and Bruce Trudgill are thanked for their constructive reviews.

References

Anders, M.H., Schlische, R.W., 1994. Overlapping faults, intrabasin highs, and the growth of normal faults. Journal of Geology 102, 165–180.

Barnes, K.R., Sneddon, J.N., McAdow, D., 1992. Integrated exploration search for additional Upper Jurassic prospectivity in the North Viking Graben, Norwegian North Sea. AAPG Annual Convention official program abstracts, P6.

Cartwright, J.A., Trudgill, B.D., Mansfield, C.S., 1995. Fault growth by segment linkage: an explanation for the scatter in maximum displacement and trace length data from the canyonlands grabens of SE Utah. Journal of Structural Geology 17, 1319–1326.

Cartwright, J.A., Mansfield, C., Trudgill, B., 1996. The growth of normal faults by segment linkage. In: Buchanan, P.G., Nieuwland, D.A. (Eds.), Modern Developments in Structural Interpretation, Validation and Modelling. Geological Society of London Special Publication 99, pp. 163–177.

Cartwright, J.A., Mansfield, C.S., 1998. Lateral displacement variations and lateral tip geometry of normal faults in the Canyonlands National Park, Utah. Journal of Structural Geology 20, 3–19.

Contreras, J., Anders, M.H., Scholtz, C.H., 2000. Growth of a normal fault system: observations from the Lake Malawi basin of the east African rift. Journal of Structural Geology 22, 159–168.

Cowie, P.A., Sornette, D., Vanneste, C., 1995. Multifractal scaling properties of a growing fault population. Geophysical Journal International 122, 457–469.

Cowie, P.A., 1998. A healing–reloading feedback control on the growth rate of seismogenic faults. Journal of Structural Geology 20, 1075–1087.

Dahl, N., Solli, T., 1993. The structural evolution of the Snorre Field and surrounding area. In: Parker, J.R. (Ed.), Petroleum Geology of Northwest Europe: Proceedings of the Fourth Conference. Geological Society of London, 1159–1166.

Dawers, N.H., Anders, M.H., Scholz, C.H., 1993. Growth of normal faults: displacement–length scaling. Geology 21, 1107–1110.

Dawers, N.H., Anders, M.H., 1995. Displacement–length scaling and fault linkage. Journal of Structural Geology 17, 607–614.

Dawers, N.H., Underhill, J.R., 2000. The role of fault interaction and linkage in controlling syn-rift stratigraphic sequences: Late Jurassic, Statfjord East Area, Northern North Sea. American Association of Petroleum Geologists Bulletin 84, 45–64.

Deegan, C.E., Scull, B.J., 1977. A standard lithostratigraphic nomenclature for the central and northern North Sea. Institute of Geological Sciences Report 77/25, 36.

Færseth, R.B., 1996. Interaction of Permo-Triasic and Jurassic extensional fault blocks during the development of the northern North Sea. Journal of the Geological Society of London 153, 931–944.

Gawthorpe, R.L., Hurst, J.M., 1993. Transfer zones in extensional basins: their structural style and influence on drainage development and stratigraphy. Journal of the Geological Society of London 150, 1137–1152.

Gawthorpe, R.L., Fraser, A.J., Collier, R.E.Ll., 1994. Sequence stratigraphy in active extensional basins: implications for the interpretation of ancient basin fills. Marine and Petroleum Geology 11, 642–658.

Gawthorpe, R.L., Sharp, I., Underhill, J.R., Gupta, S., 1997. Linked sequence stratigraphic and structural evolution of propagating normal faults. Geology 25, 795–798.

Gradstein, F.M., Agterberg, F.P., Ogg, J.P., Hardenbol, J., Van Veen, P., Thierry, J., Huang, Z., 1995. A Triassic, Jurassic and Cretaceous time scale. Geochronology, time scales and global stratigraphic correlations. SEPM Special Publication 54, 95–126.

Gudmundsson, A., 1987a. Geometry, formation and development of tectonic fractures on the Reykjanes Peninsula, southwest Iceland. Tectonophysics 139, 295–308.

Gudmundsson, A., 1987b. Tectonics of the Thingvellir fissure swarm, SW Iceland. Journal of Structural Geology 9, 61–69.

Gupta, S., Cowie, P.A., Dawers, N.H., Underhill, J.R., 1998. A mechanism to explain rift-basin subsidence and stratigraphic patterns through fault-array evolution. Geology 26, 595–598.

Haram, L., Johannessen, E.P., Syrstad, E., Kenshaw, D.K., 1990. A subtle Upper Jurassic stratigraphic trap in the northern North Sea: an exploration case history. European Association of Petroleum Geoscientists Third Conference and Technical Exhibition, p. E6.

Hardy, S., McClay, K., 1999. Kinematic modelling of extensional fault-propagation folding. Journal of Structural Geology 21, 695–702.

Hollander, N.B., 1987. Snorre. In: Spencer, A.M., Campbell, C.J., Hanslien, S.H., Holter, E., Nelson, P.H.H., Nysæther, E., Ormaasen, E.G. (Eds.). Geology of the Norwegian Oil and Gas Fields. Graham and Trotman, London, pp. 307–318.

Jackson, J.A., White, M.J., Garfunkel, Z., Anderson, H., 1988. Relations between normal-fault geometry, tilting and vertical motions in extensional terrains: an example from the southern Gulf of Suez. Journal of Structural Geology 10, 155–170.

McLeod, A., Underhill, J.R., 1999. Processes and products of footwall degradation, northern Brent Field, northern North Sea. In: Fleet, A.J., Boldy, A.A.R. (Eds.), Petroleum Geology of Northwest Europe: Proceedings of the Fifth Conference. Geological Society of London, pp. 91–106.

Nicol, A., Walsh, J.J., Watterson, J., Underhill, J.R., 1997. Displacement rates on normal faults. Nature 390, 157–159.

Nøttvedt, A., Berge, A.M., Dawers, N.H., Færseth, R.B., Hager, K.O., Mangerud, G., Puigdefabregas, C., 2000. Syn-rift evolution and resulting play models in the Snorre-H area, northern North Sea. In: Nøttvedt, A. (Ed.), Dynamics of the Norwegian Margin. Geological Society of London Special Publication 167, 179–218.

Peacock, D.C.P., Sanderson, D.J., 1991. Displacements, segment linkage and relay ramps in normal fault zones. Journal of Structural Geology 13, 721–733.

Rattey, R.P., Hayward, A.B., 1993. Sequence stratigraphy of a failed rift system: the middle Jurassic to early Cretaceous basin evolution of the central and northern North Sea. In: Parker, J.R. (Ed.), Petroleum Geology of Northwest Europe: Proceedings of the Fourth Conference. Geological Society of London, pp. 215–249.

Ravnås, R., Bondevik, K., 1997. Architecture and controls on Bathonian to Kimmeridgian shallow-marine syn-rift wedges in the Oseberg–Brage area, northern North Sea. Basin Research 9, 197–226.

Ravnås, R., Bondevik, K., Helland-Hansen, W., Lømo, L., Ryseth, A., Steel, R.J., 1997. Sedimentation history as an indicator of rift initiation and development: the Late Bajocian–Bathonian evolution of the Oseberg–Brage area, northern North Sea. Norsk Tidsskrift 77, 205–232.

Roberts, A.M., Yielding, G., Kuznir, N.J., Walker, I., Dorn-Lopez, D., 1993. Mesozoic extension in the North Sea: constraints from flexural backstripping, forward modelling and fault populations. In: Parker, J.R., (Ed.), Petroleum Geology of Northwest Europe: Proceedings of the Fourth Conference. Geological Society of London, pp. 1123–1136.

Rowan, M.G., Hart, B.S., Nelson, S., Flemings, P.B., Trudgill, B.D., 1998. Three-dimensional geometry and evolution of a salt-related growth-fault array: Eugene Island 330 field, offshore Louisiana, Gulf of Mexico. Marine and Petroleum Geology 15, 309–328.

Sahagian, D., Pinous, O., Olferiev, A., Zakharov, V., 1996. Eustatic curve for the Middle Jurassic–Cretaceous based on Russian Platform and Siberian stratigraphy: zonal resolution. American Association of Petroleum Geologists Bulletin 80, 1433–1458.

Schlische, R.W., 1995. Geometry and origin of fault related folds in extensional settings. American Association of Petroleum Geologists Bulletin 79, 1661–1678.

Schlische, R.W., Anders, M.H., 1996. Stratigraphic effects and tectonic implications of the growth of normal faults and extensional basins. In: Beratan, K.K. (Ed.), Reconstructing the History of Basin and Range Extension Using Sedimentology and Stratigraphy. Geology Society of America, Special Papers 33, 183–203.

Schlische, R.W., Young, S.S., Ackermann, R.V., Gupta, A., 1996. Geometry and scaling relations of a population of very small rift-related normal faults. Geology 24, 683–686.

Trudgill, B.D., Cartwright, J.A., 1994. Relay-ramp forms and normal fault linkages, Canyonlands National Park, Utah. American Association of Petroleum Geologists Bulletin 106, 1143–1157.

Underhill, J.R., 1991. Controls on late Jurassic seismic sequences, Inner Moray Firth, UK North Sea: a critical test of a key segment of Exxon's original global cycle chart. Basin Research 3, 79–98.

Underhill, J.R., Partington, M.A., 1993. Jurassic thermal doming and deflation in the North Sea: implications of the sequence stratigraphic evidence. In: Parker, J.R. (Ed.), Petroleum Geology of Northwest Europe: Proceedings of the Fourth Conference. Geological Society of London, pp. 337–346.

Underhill, J.R., Sawyer, M.J., Hodgson, P., Shallcross, M.D., Gawthorpe, R.L., 1997. Implications of fault scarp degradation for Brent Group prospectivity, Ninian Field, northern North Sea. American Association of Petroleum Geologists Bulletin 81, 999–1022.

Underhill, J.R., 1998. Jurassic. In: Glennie, K.W. (Ed.). Petroleum Geology of the North Sea. Blackwell Science, London, pp. 245–293.

Willemse, E.J.M., Pollard, D.D., Aydin, A., 1996. Three-dimensional analysis of slip distribution on normal fault arrays with consequences of fault scaling. Journal of Structural Geology 18, 295–310.

Withjack, M.O., Olson, J., Peterson, E., 1990. Experimental models of extensional forced folds. American Association of Petroleum Geologists Bulletin 74, 1038–1054.

Wood, J., Schwartzbard, A.E., 1994. Upper Jurassic lowstand and highstand systems tracts on the dip slope of Snorre–Vidgis–Tordis mega footwall. European Association of Petroleum Geoscientists Sixth Conference and Technical Exhibition, CO43.

Yielding, G., 1990. Footwall uplift associated with Late Jurassic normal faulting in the northern North Sea. Journal of the Geological Society of London 147, 219–222.

Yielding, G., Badley, M.E., Roberts, A.M., 1992. The structural evolution of the Brent Province. In: Hazeldine, A.C., Giles, R.S., Brown, S. (Eds.), Geology of the Brent Group. Geological Society of London Special Publication 71, pp. 35–66.